2007 IEEE International Conference on
Robotics and Automation
Roma, Italy, 10-14 April 2007

Autonomously Flying VTOL-Robots: Modeling and Control

Konstantin Kondak, Markus Bernard, Nicolas Meyer, Günter Hommel

Technische Universität Berlin,
Real-Time Systems and Robotics Group,
Faculty of Electrical Engineering and Computer Science
Einsteinufer 17/EN10, Berlin 10587

***Abstract*— In this paper an approach for control of autonomously flying robots with vertical take off and landing capabilities (VTOL) is presented. After reviewing that the motion description for different VTOL-robots is very similar, the general control scheme for VTOL-robots is presented. This scheme is based on linearisation and decoupling using inversion of the system model blocks. To compensate the model uncertainties and disturbances two additional parts are included into the controller: a reduced state observer based on a robot motion model as well as a disturbances observer and compensator for orientation control. The presented approach was applied to two different VTOL-robots: a helicopter and a quad-rotor. In real flight experiments it was verified that the presented general but simple controller provides sufficient performance for a wide range of practical applications.**

I. Introduction

Autonomously flying robots or Unmanned Aerial Vehicles (UAV), equipped with different sensors, can be used in many practical applications e.g. inspections, filming, deploying sensor networks etc. In this paper, we address small size VTOL-robots (up to 20 kg), see scheme in Fig. 1, which can produce the lifting force $\mathbf{F}_3$ and three torques $\mathbf{T}_{1,2,3}$ independently. The forces $\mathbf{F}_{1,2}$ can be also produced by the robot, but they are not required to be independent of $\mathbf{F}_3$ and $\mathbf{T}_{1,2,3}$. The most common examples of this class of VTOL-robots are helicopters and quad-rotors.

There are many publications where important aspects of modeling and control for small size helicopters are revealed, see e.g. [1]–[3]. But one aspect of modeling is not covered in the most of them: the inertial (gyroscopic) effects of the main rotor which affect the behavior of the mechanical model. For commercially available small size helicopters (without bulky equipment fixed to the fuselage as shown in Fig. 8) the following simple model approximates the behavior of the whole system very well: a thin spinning disc (for the main rotor) with a mass point (for the fuselage) in the middle, see also our previous work [4], [5]. This important aspect is not addresed in some papers probably because the authors wanted to utilize the results achieved for full size helicopters without necessary adaptation.

There are also many publications where modeling and control of quad-rotors are explained, see e.g. [3], [6]. Most of them use the Draganflyer (a small, remote controlled, commercially available quad-rotor toy) as basic platform. The Draganflyer has an integrated PI-controller for rotation stabilization. Many groups use the existing control interface of the Draganflyer and therefore the integrated PI-controller. In this work, both the stabilization of the orientation and the control of translation are considered. The quad-rotor described in this paper with a mass of 5 kg belongs to an other weight class than the Draganflyer and is the heaviest autonomously flying quad-rotor with electrical motors and fixed pitches known to the authors.

In this paper we show that the motion description for different types of VTOL-robots is similar, Sec. II. After that, the general control approach for VTOL-robots will be presented, Sec. III. This approach is based on model linearisation by means of inverse kinematics and dynamics. A reduced state observer for estimation of the robot attitude (roll and pitch angles) is presented in Sec. IV-A. The problem of attitude estimation was studied by other groups before from different perspectives: E.g. in [7] a fusion algorithm between the data of gyroscopes and a delayed orientation data obtained from an off-board vision system is studied. Another approach is to fuse measurements taken from different inertial sensors, as in [8] the data of gyroscopes and accelerometers and in [9] of gyroscopes and inclinometers are used to estimate the attitude. In contrast to other studies the presented state observer is based on the motion description (translation and rotation) of the VTOL-robot and needs only the robot position, its translation velocity and rotation speeds as input. The forces and torques generated by the robot are chosen as abstract system inputs. This allows us to consider the modeling and control of different VTOL-robots in a general way. In Sec. IV-B the conversion from abstract to real system inputs is explained. To compensate for model uncertainties and disturbances from outside the mentioned reduced state observer as well as the disturbances observer and compensator, described in Sec. IV-C, are used. The presented approach was applied to two VTOL-robots: a helicopter and a quad-rotor. For both types of robots the performance of the presented approach was verified in real flight experiments, Sec. V. Conclusions are drawn in Sec. VI.

From our experience we can not confirm that control of VTOL-robots belonging to the defined class requires complex non-linear and/or adaptive techniques, at least if the controller performance demonstrated in Sec. V is sufficient. In our experiments the same controller has performed well in different flight modes: take off, landing, hovering, forward flight. Therefore we think also that for the defined class of

1-4244-0602-1/07/$20.00 ©2007 IEEE.

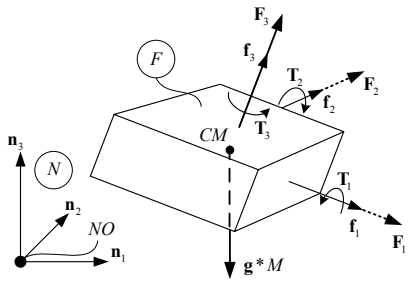

Fig. 1. The scheme of the considered class of VTOL-robots.

VTOL-robots there is no need to design different models and different types of controllers for each of these flight modes. We will try to explain our point of view on the control problem for the considered class of robots and will show the main common issues and main differences to the work which can be found in the literature.

II. Modeling

The model of the considered VTOL-robots is composed of two main components: the mechanical model and the model for generation of aerodynamic forces and torques. From experimental results with helicopters and quad-rotors we concluded that the generation of aerodynamic forces and torques, at least for VTOL-robots under 20 kg, can be approximated with simple algebraic relations. Therefore, the dynamics of the system are mostly determined by its mechanical model. $\mathbf{F}_3$ and $\mathbf{T}_{1,2,3}$ will be considered as abstract system inputs. In Sec. IV-B the conversion from abstract to real system inputs will be explained.

A. Kinematics

We introduce six generalized coordinates q_i, $i = 1, \ldots, 6$ and six generalized velocities u_i, $i = 1, \ldots, 6$. The generalized coordinates $q_{1,2,3}$ describe the position of the reference point CM (center of mass) and the generalized velocities $u_{1,2,3}$ – its motion in an inertial frame N. The generalized coordinates $q_{4,5,6}$ are Euler-angles defined about axes $\mathbf{f}_{1,2,3}$ describing the orientation of the fuselage or of the frame F in N. The angular velocity of the frame F in N is described by means of generalized velocities $u_{4,5,6}$: $\boldsymbol{\omega}_{F-N} = u_4\mathbf{f}_1 + u_5\mathbf{f}_2 + u_6\mathbf{f}_3$. This definition of generalized coordinates and velocities yields the following kinematic equations for translation: $\dot{q}_{1,2,3} = u_{1,2,3}$, and for rotation:

$$\begin{aligned} \dot{q}_4 &= (u_4 \cos(q_6) - u_5 \sin(q_6)) / \cos(q_5) \\ \dot{q}_5 &= u_4 \sin(q_6) + u_5 \cos(q_6) \\ \dot{q}_6 &= u_6 + \tan(q_5)(u_4 \cos(q_6) - u_5 \sin(q_6)) \end{aligned} \quad (1)$$

B. Translation dynamics

The following equations describe the translation dynamics of the reference point CM in frame N:

$$\begin{pmatrix} \dot{u}_1 \\ \dot{u}_2 \\ \dot{u}_3 \end{pmatrix} M = C_{f-n} \begin{pmatrix} F_1 \\ F_2 \\ F_3 \end{pmatrix} + \begin{pmatrix} 0 \\ 0 \\ -g * M \end{pmatrix} \quad (2)$$

where C_{f-n} is the orientation matrix of the frame F relative to N and M is the mass of the whole system.

C. Rotation dynamics for a helicopter

The mechanical model of a helicopter is composed of three rigid bodies: fuselage, main rotor and tail rotor. In [4], [5] the authors presented the contribution estimation of these three rigid bodies to the rotation dynamics. The result was that for almost all commercially available small size helicopters the following is true: due to the dominance of the inertial effects of the spinning main rotor only the main rotor should be considered as a rigid body in equations for rotation dynamics; the fuselage can be modeled as a mass point and the mass of the tail rotor can be simply neglected. Only if some devices with a distributed mass, like a safety cage as shown in Fig. 8, *dramatically* increase the inertial numbers of the fuselage, the fuselage should be considered as a rigid body like the main rotor.

The rotation dynamics for a general model composed of two rigid bodies (fuselage and main rotor) have the following form:

$$T_1 + (K_{156}u_6 + K_{15})\, u_5 + K_{1p4}\dot{u}_4 = 0 \quad (3)$$

$$T_2 + (K_{246}u_6 + K_{24})\, u_4 + K_{2p5}\dot{u}_5 = 0 \quad (4)$$

$$T_3 + K_{345}u_4u_5 + K_{23}\dot{u}_6 = 0. \quad (5)$$

The constant coefficients K_{xxx} depend on helicopter parameters as well as on rotation speed of the main rotor and are explained in [4].

To simplify the analysis of rotation dynamics and controller design the following assumption will be made:

$$u_6 = const. \quad (6)$$

This assumption means that in each flight maneuver the rotation speed around vertical fuselage axis $\mathbf{f}_3$ is zero or constant. This can be achieved by using a separate control loop for u_6. In Eq. (5) the torque T_3 can be expressed as follows: $T_3 = F_2^{TR} * L + T_3^{MR}$. The force F_2^{TR} generated by the tail rotor, will be exclusively used as input to control u_6 (L is the distance between the main and tail rotor shafts). The drag torque of the main rotor T_3^{MR} and the term $K_{345}u_4u_5$ will be considered as disturbances. Eq. (5) shows that, regarding F_2^{TR}, u_6 behaves like a simple integrator and therefore can be easily controlled with a PI-controller.

Due to assumption (6) the rotation dynamics for axes $\mathbf{f}_{1,2}$ can be treated independent from rotation about axis $\mathbf{f}_3$, and as Eqs. (3), (4) show, is linear.

As mentioned above, for most of small size helicopters the inertial effects of the fuselage can be neglected if the rotation dynamics are considered. The analysis of Eqs. (3), (4) shows, see [4], [5], that for this case, the rotation dynamics for axes $\mathbf{f}_{1,2}$ can be well approximated with the following simple algebraic relations:

$$u_4 = -\frac{1}{2\, I_{11}^{MR}\omega_{MR}}\, T_2; \quad u_5 = \frac{1}{2\, I_{11}^{MR}\omega_{MR}}\, T_1, \quad (7)$$

where I_{11}^{MR} is the inertia number of a solid disc with the same mass distribution as a spinning rotor with respect to the center of mass and to an axis which is perpendicular to the rotation axis of the rotor; ω_{MR} is the rotation speed of the main rotor.

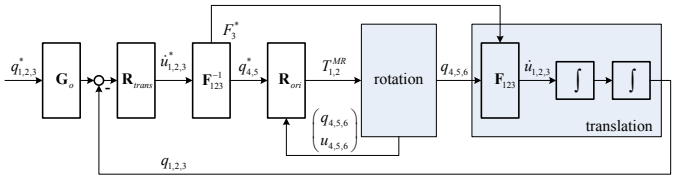

Fig. 2. Translation control.

D. Rotation dynamics for quad-rotor

The mechanical model of the quad-rotor is composed of five rigid bodies: four rotors and a fuselage. Two rotors have positive and two have negative rotation speed. Due to the compensation of contributions from the first two rotors by the second two rotating in the opposite direction, the rotation dynamics for the considered quad-rotor are given mostly by the inertial effects of the fuselage and is well approximated by Euler equations:

$$T_1 \quad +(I_{33}-I_{22})u_5u_6 - I_{11}\dot{u}_4 = \quad 0 \tag{8}$$

$$T_2 \quad -(I_{33}-I_{11})u_4u_6 - I_{22}\dot{u}_5 = \quad 0 \tag{9}$$

$$T_3 \quad +(I_{22}-I_{11})u_4u_5 - I_{33}\dot{u}_6 = \quad 0 \tag{10}$$

where I_{ii}, $i = 1,2,3$, are the inertia numbers with respect to the center of mass and the axes $\mathbf{f}_{1,2,3}$. Like in case of the helicopter, we assume that u_6 will be controlled by a separate control loop so that (6) holds, and the rotation dynamics of the quad-rotor can be considered as linear.

III. Control

The motion of the considered VTOL-robots is controlled by adjusting the orientation of the robot (or direction of the force $\mathbf{F}_3$) and the value of F_3. This control scheme is shown in Fig. 2. The inputs are the desired position $q^*_{1,2,3}$ and velocity $u^*_{1,2,3}$ of the robot's reference point. As mentioned in Sec. II-C and II-D the orientation control for axis $\mathbf{f}_3$ is performed using a separate control loop. This control loop is not shown in Fig. 2. The control scheme in Fig. 2 is composed of inner and outer loops. The outer loop controller $\mathbf{R}_{trans}$ uses the position and velocity errors as inputs and calculates the needed translational accelerations in order to reduce these errors. The resulting accelerations are converted into the orientation of the robot plane $q^*_{4,5}$ and value of the lifting force $\mathbf{F}_3$ in the block $\mathbf{F}^{-1}_{123}$. The orientation of the robot plane is controlled in the inner loop by means of controller $\mathbf{R}_{ori}$ which computes the input torques T_1 and T_2.

A. Translation control

As can be seen in Fig. 2, the translation controller is composed of two blocks: $\mathbf{F}^{-1}_{123}$ and $\mathbf{R}_{trans}$. The equations for the block $\mathbf{F}^{-1}_{123}$ can be found by solving Eqs. (2) for $q^*_{4,5}$ and F_3 with assumption that $F_{1,2} = 0$:

$$F_3 = M\sqrt{\dot{u}_1^2 + \dot{u}_2^2 + (\dot{u}_3 + g)^2}$$

$$q_5 = \arcsin(M\frac{\dot{u}_1}{F_3})$$

$$q_4 = -\arcsin(M\frac{\dot{u}_2}{F_3\cos(q_5)})$$

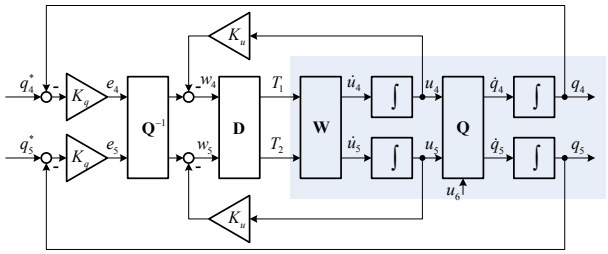

Fig. 3. Control of orientation angles $q_{4,5}$.

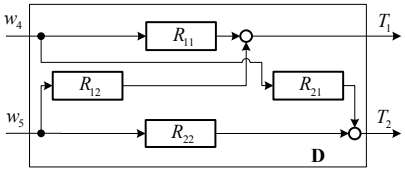

Fig. 4. The structure of the decoupling block $\mathbf{D}$.

For the block $\mathbf{R}_{trans}$ a simple PID-controller is used. The calculation of the coefficients for this PID-controller is explained in Sec. III-C.

B. Orientation control for axis $\mathbf{f}_{1,2}$

The scheme for the control of orientation angles $q_{4,5}$ is shown in Fig. 3. The controller is composed of blocks $\mathbf{Q}^{-1}$, $\mathbf{D}$ and two feedback loops with gains K_u, K_q for rotation speeds $u_{4,5}$ and orientation angles $q_{4,5}$ respectively. The rotation dynamics for axes $\mathbf{f}_{1,2}$ are described by Eqs. (3), (4) or by Eqs. (8), (9). In Fig. 3 these equations are represented by the block $\mathbf{W}$. The block $\mathbf{D}$ of the controller is used to decouple the plant between $T_{1,2}$ and $u_{4,5}$. This decoupling can be performed by means of known techniques from linear control theory. In this work block $\mathbf{D}$ was computed in such a way that the decoupled plant between $w_{4,5}$ and $u_{4,5}$ becomes equivalent to two independent integrators. This allows the usage of an additional feedback loop based on a simple P-controller with gain K_u to control $u_{4,5}$, as shown in Fig. 3. The structure of the decoupling block $\mathbf{D}$ is shown in Fig. 4. The transfer functions R_{ij} for the helicopter are computed using Eqs. (3), (4) with $u_6 = 0$ and have the following form:

$$R_{11} = -K_{1p4};\ R_{12} = -\frac{K_{15}}{s};\ R_{21} = -\frac{K_{24}}{s};\ R_{22} = -K_{2p5} \tag{11}$$

In the same way the transfer functions R_{ij} for the quad-rotor are computed using Eqs. (8), (9) :

$$R_{11} = I_{11};\ R_{12} = R_{21} = 0;\ R_{22} = I_{22} \tag{12}$$

The block $\mathbf{Q}^{-1}$ inverts the kinematics of the robot. The equations for this block are obtained by solving the first two equations in (1) for $u_{4,5}$.

If a helicopter without bulky equipment fixed to the fuselage is used, the rotation dynamics are described by Eqs. (7) and the control of $q_{4,5}$ can be simplified even more: Due to Eqs. (7) and $\mathbf{Q}\mathbf{Q}^{-1} = \mathbf{1}$, the plant between $e_{4,5}$ and $q_{4,5}$ in Fig. 3 is equivalent to two parallel integrators. Therefore the control of orientation angles $q_{4,5}$ can be achieved with a P-controller, and the inner feedback loops with the gains K_u can be omitted.

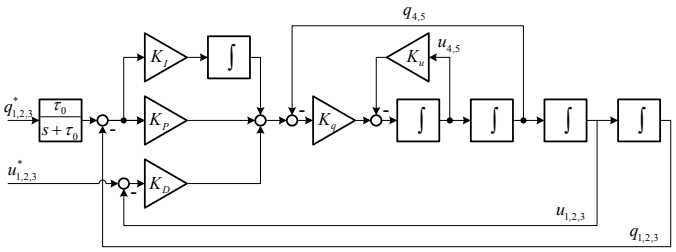

Fig. 5. The scheme of the closed loop system for calculation of the controller coefficients.

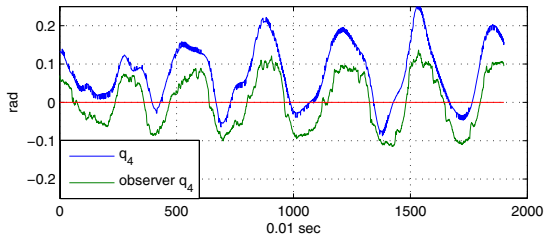

Fig. 6. Estimated and real orientation angle q_4 of the helicopter recorded in an autonomous flight.

C. Calculation of the controller coefficients

After inserting the content for blocks $\mathbf{R}_{trans}$, $\mathbf{F}_{123}^{-1}$ and $\mathbf{R}_{rot}$ in Fig. 2, the general control scheme can be represented with a linear system shown in Fig. 5. K_P, K_I and K_D are the gains of the PID-controller from the block $\mathbf{R}_{trans}$; K_q, K_u are the gains of the orientation controller for $q_{4,5}$, and τ_0 is the time constant of the prefilter $\mathbf{G}_0$. The unknown coefficients K_P, K_I, K_D, K_q and K_u can be calculated using methods of the linear control theory. In this paper, the simple pole assignment method was used. The time constant τ_0 of the prefilter could be chosen according to the rule $\tau_0 = \tau_{sys}/5$.

IV. Implementation of the Controller

A. State observer

The two reasons for using a state observer are: determination of state variables which can not be measured directly, and adjustment of the state variables to the model which was used for the controller design. The usage of a similar system model in the state observer as for the controller design corrects the state variables in such a way that the system behavior appears to the controller closer to the behavior of the model used for its design. In some cases this allows to increase the performance of the closed loop system.

We used the reduced Luenberber observer to determine the orientation angles $q_{4,5}$. For that Eqs. (1) and (2) are linearized in the point $q_{4,5,6} = 0$. The observer inputs are $q_{1,2}$, $u_{1,2}$, $u_{4,5}$ and its outputs – $q_{4,5}$. For computation of the observer gain matrix $\mathbf{L}$, the observer poles should be specified. The limit for the increasing of the observer poles (or increasing the gains in $\mathbf{L}$) is given by the measurement noise of the observer inputs. To be able to rotate the robot about the vertical axis $\mathbf{f}_3$ we have to transform the observer inputs into a coordinate system in which the angle q_6 is always 0. Fig. 6 shows the observed and directly measured (possible with our motion tracking system) angle q_4 from a real flight experiment with a helicopter, see Sec. V for more details about experiments and observer parameters.

In Fig. 6 we can see why the observer can improve the controller performance. The tail rotor of the helicopter produces a force $\mathbf{F}_2$ which tries to move the helicopter sidewards and should be compensated in hover configuration by the roll angle q_4 (note that the mean value of measured q_4 in Fig. 6 is not zero). In contrast to the direct measurement, the observer calculates the angle q_4 considering the motion of the system. That means that in the hovering mode, where no translation is performed, the projection of the lifting force $\mathbf{F}_3$ onto the axis $\mathbf{n}_2$ and therefore also the observed angle q_4 will be zero. The measured value of q_4 does not fit the model which was used for controller design and therefore this discrepancy in q_4 should be compensated by the controller. The mean value of q_4 calculated by the observer is approximately zero.

The second advantage of this observer is that only the gyroscopes are needed to determine the orientation angles $q_{4,5}$. Therefore no accelerometers are needed and the IMU of the robot can be simplified compared to the usual approach to compute $q_{4,5}$ using both the gyroscopes and accelerometers. Of course, the presented observer requires the determination of the robot position.

B. Calculation of the real input signals

The abstract system inputs (or controller outputs) $T_{1,2,3}$ and F_3 should be recalculated into the real system inputs. Our helicopter, see Fig. 8, has a 120° swash-plate with three points. The real input are the four servo signals S_{xxx}:

$$\begin{aligned} S_{nick} &= F_3 * k_{col} + T_1 * k_{cyc} + \triangle_{nick} \\ S_{rl} &= F_3 * k_{col} - 0.5 * T_1 * k_{cyc} + T_2 * k_{cyc} + \triangle_{rl} \\ S_{rr} &= F_3 * k_{col} - 0.5 * T_1 * k_{cyc} - T_2 * k_{cyc} + \triangle_{rr} \\ S_{tail} &= T_3 * k_{tail} + \triangle_{tail}. \end{aligned} \tag{13}$$

The subscripts denote the corresponding servo (rl denotes roll left, rr roll right, $nick$ nick, col collective and cyc cyclic). The constant coefficients k_{xxx} and constant offsets $\triangle_{xxx}$ are found by experiments. In the last equations the aerodynamics and the non-linearities in the lever connections between servos and rotor blades are approximated with simple linear functions. The experiments show, that this simple approximation works well in the relevant operation range. The elaborated modeling of the effects on the main rotor is problematic (among other things because of the unknown Bell-Hiller bar motion which depends on several unknown parameters) and, to our experience, does not improve the controller performance.

Our quad-rotor, see Fig. 9, is driven by four motors with fixed pitch propellers. The real system inputs are the signal for the motor controllers, see also Sec. V. First the four forces $f_{1,2,3,4}$ to be generated by the propellers are calculated:

$$\begin{aligned} f_1 &= F_3/4 - k_{T12} * T_2 + k_{T3} * T_3 \\ f_2 &= F_3/4 + k_{T12} * T_1 - k_{T3} * T_3 \\ f_3 &= F_3/4 + k_{T12} * T_2 + k_{T3} * T_3 \\ f_4 &= F_3/4 - k_{T12} * T_1 - k_{T3} * T_3. \end{aligned} \tag{14}$$

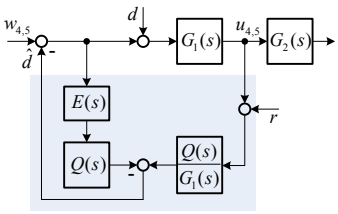

Fig. 7. Scheme for the disturbances observer and compensator.

From the forces $f_{1,2,3,4}$ the rotation speeds $\omega_{1,2,3,4}$ of the motors are calculated: $\omega_{1,2,3,4} = k_\omega * \sqrt{f_{1,2,3,4}}$. After that the signals for the motor controllers are generated as follows: $S_{1,2,3,4} = k_m * \omega_{1,2,3,4} + \triangle_m$. The constant coefficients k_{T12}, k_{T3}, k_ω, k_m and $\triangle_m$ were determined by experiments.

C. Model uncertainties and disturbances

The presented control approach is based on the inversion of the system non-linearities. In several papers the usage of such inversions is claimed to be sensitive to parameter uncertainties of the system. For that reason, more complicated non-linear methods or/and parameter estimation techniques are considered. Analyzing our experiments we can not confirm this point of view.

As explained above, the non-linearities of the model are compensated by blocks $\mathbf{F}_{123}^{-1}$ and $\mathbf{Q}^{-1}$. The block $\mathbf{Q}^{-1}$ contains only the geometrical relationships describing the orientation of the frame F relative to frame N and is independent of any system parameters. Of course, this compensation does not work if the orientation angles can not be measured or observed properly. The same argumentation can be applied for compensation of $\mathbf{F}_{123}$ with $\mathbf{F}_{123}^{-1}$. The only one system parameter in $\mathbf{F}_{123}^{-1}$ is the system mass which can be easily measured precisely enough. In our opinion the elements of the system model described in Sec. II and III do not need to be estimated, and can be taken from the presented model.

As explained in Sec. IV-B, the calculation of the real input signals from the computed abstract inputs F_3, $T_{1,2,3}$ is done by means of rough approximations which cause the discrepancies between the system model and the real system. To deal with these rough approximation and disturbances from outside a disturbances observer and compensator can be used. Inspired by work [10], a well known common scheme shown in Fig. 7 was applied to our systems. The observer and compensator are denoted by the gray rectangle, $G_1(s)G_2(s)$ is the transfer function of the system. The disturbances and influences from parameter uncertainties are modeled by means of the unknown signal d acting on the system input; r is a measurement noise. The signal $\hat{d}$ is the observed disturbance which is used as a correction for the actual system input $w_{4,5}$. $Q(s)$ is a low pass filter and $E(s)$ the estimated time delay neglected by modeling the system part $G_1(s)$. Theoretically the disturbances observer and compensator in Fig. 7 can be used before each inversion block, if the corresponding reference signal $u_{4,5}$ is available. The presented equations for generation of F_3 and $T_{1,2,3}$, Eqs. (13) and (14), are the most inaccurate part of the system model. Therefore the disturbances observer should be used before the blocks $\mathbf{D}$ and $\mathbf{F}_{123}^{-1}$, see Fig. 3 and 2. In our experiments the usage of the disturbances observer before the block $\mathbf{D}$ (generation of $T_{1,2}$) has improved the controller performance, especially for the quad-rotor. For that case we have: $G_1(s) = 1/s$, $Q(s) = 1/(Ts + 1)$ where T is a small constant. The compensation of disturbances and system uncertainties before block $\mathbf{F}_{123}^{-1}$ has not increased the system performance notably.

Fig. 8. Helicopter during autonomous flight.

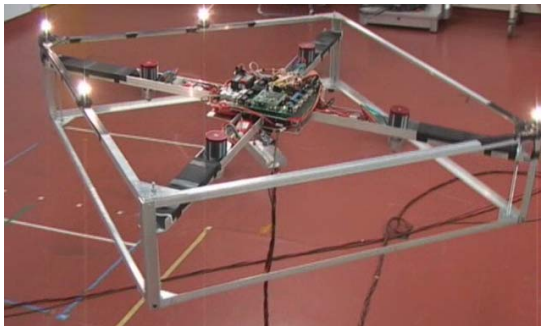

Fig. 9. Quad-rotor during autonomous flight.

V. Experimental results

The presented control approach was verified in real flight experiments with two types of VTOL-robots: a helicopter and a quad-rotor.

In Fig. 8 the electrical model helicopter Logo14 rigidly fixed in a safety cage (made of carbon tubes, mass ca. 1.2 kg) is shown. The diameter of the main rotor of the helicopter is 1.1 m and the total weight of the system with safety cage is about 4.8 kg. The helicopter is equipped with the commercial gyroscope based controller GY401 for u_6 as well as with the motor speed controller Jazz 55-10-32 which ensures constant rotation speed of the main rotor. The presented experiments were carried out with $\omega_{mr} = 2000$ rpm.

In Fig. 9 our quad-rotor is shown. It is composed of an aluminum frame with dimensions $0.8 \times 0.8 \times 0.2$ m, four brushless motors Kontronik KORA 25-16, each driven by the controller Jazz 55-10-32 with switched off rotation speed control mode and of four fixed pitch propellers with the diameter of 39 cm. The mass of the quad-rotor is about 5 kg.

In the conducted flight experiments the position of VTOL-robots was determined by an optical motion tracking system, designed in our group. The translation velocities were determined by first order differentiation of the corresponding coordinates. The angular speeds $u_{4,5}$ were measured by onboard

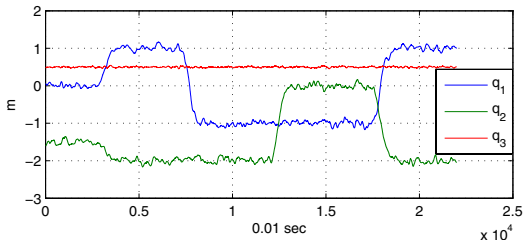

Fig. 10. Position of the quad-rotor during the test flight.

gyroscopes ADXRS 300. The orientation angles $q_{4,5}$ were calculated using a state observer described in Sec. IV-A. The motion-tracking system calculates all three orientation angles $q_{4,5,6}$: q_6 was used for control, $q_{4,5}$ only as reference signals for the assessment of the state observer.

The performance of the proposed control approach is illustrated in Fig. 10, where the most difficult case – the position control – is shown (compared to velocity control). The Fig. 10 shows the test flight of the quad-rotor. In this test flight the desired position of the quad-rotor was several times changed with a step function. The desired coordinates were changed as follows: $q_{1,2}$ simultaneously, then q_1, after that q_2 and again $q_{1,2}$ simultaneously. The altitude q_3 had to be constant during the whole flight. The desired positions are reached in a specified time with zero offset. The maximal deviation from the desired value is ca. $10\,\text{cm}$. The curves for the helicopter flight are very similar to those in Fig. 10 and therefore are not shown here. For both robots the poles of the closed loop system were specified at -1. The poles of the observer for helicopters are set to -10 and for the quad-rotor to -3 (due to the larger noise of gyroscopes). The constant T in the disturbances observer described in Sec. IV-C was set to 0.02 for the quad-rotor and the time delay in $G_1(s)$, see Fig. 7, was estimated with $150\,\text{ms}$. The disturbances observer for the helicopter has not increased the performance significantly.

In the conducted flight experiments we could verify that the helicopter and the quad-rotor can be controlled with the same control approach presented in Sec. III. The reduced observer, presented in Sec. IV-A, works well with both systems, but especially for the helicopter it increases significantly the position tracking performance. The disturbances observer has also improved the controller performance, especially for the quad-rotor. The controller seems to be robust to the parameter variation of the systems as well as of the controller itself. On the other hand we were not able to achieve positioning precision better than $0.1\,\text{m}$. At the moment we are not sure of the main reason for this limit. But this precision is sufficient for most practical applications. The coefficients in approximations (13) and (14) for the calculation of the real system inputs could also be changed in some range and therefore can be easily determined in experiments.

VI. Conclusion

In this paper it was shown that for a large class of flying VTOL-robots a quite simple general approach for modeling and control leads to performance which is sufficient for most practical applications. Based on experimental results (not presented in this paper) it was stated that the aerodynamics can be adequately approximated with linear functions and that the behavior of the considered VTOL-robots is essentially determined by their mechanical model. It was reviewed, that under weak assumptions about the rotation speed about the vertical axis, the rotation dynamics of the mechanical model are linear. The kinematic equations of rotation are highly non-linear. But these non-linearities originate from the geometrical transformation of vectors from the robot into the inertial frame. These non-linearities do not depend on robot parameters and, therefore, their inversion can be used for compensating these non-linearities even if the parameters of the system are unknown. A state observer for orientation angles was presented. This observer calculates the pitch and roll angles without using accelerometers, in contrast to commonly used IMU-devices. It was shown, that using this state observer the performance of the closed loop system is increased. The rough approximations modeling the generation of aerodynamic forces, as well as the non-modeled influences from outside were compensated by the additional disturbances observer and compensator.

The methods and algorithms presented in this paper were verified in flight experiments using VTOL-robots with all six degrees of freedom. Practical issues, like sensor noise, input limits, etc., are very important for the assessment of different control methods for VTOL-robots. Very often the experiments using robots with some fixed degrees of freedom do not reveal relevant aspects of the problem. In general, fixing of some degrees of freedom means reducing the order of the system and therefore oversimplifies the problem.

References

[1] B. M. V. Gavrilets and E. Feron, "Non-linear model for a small-size acrobatic helicopter," in *AIAA Guidance, Navigation and Control Conference*, August 2001.

[2] S. K. Kim and D. M. Tilbury, "Mathematical modeling and experimental identification of an unmanned helicopter robot with flybar dynamics," *Journal of Robotic Systems*, vol. 21, no. 3, pp. 95–116, 2004.

[3] P. Castillo, R. Lozano, and A. E. Dzul, *Modelling and Control of Mini-Flying Machines*. Springer, 2005.

[4] K. Kondak, M. Bernard, N. Losse, and G. Hommel, "Elaborated modeling and control for autonomous small size helicopters," in *ISR/ROBOTIK 2006 Joint conference on robotics*, 2006.

[5] K. Kondak, C. Deeg, G. Hommel, M. Musial, and V. Remuß, "Mechanical model and control of an autonomous small size helicopter with a stiff main rotor," in *IEEE/RSJ Int. Conf. on Intelligent Robots and Systems*, 2004.

[6] G. Hoffmann, D. Rajnarayan, S. Waslander, D. Dostal, J. Jang, and C. Tomlin, "The stanford testbed of autonomous rotorcraft for multi agent control (starmac)," in *The 23rd Digital Avionics Systems Conference*, 2004.

[7] M. Earl and R. D'Andrea, "Real-time estimation techniques applied to a four-rotor helicopter," in *IEEE Int. Conf. on Decision and Control*, 2004.

[8] N. Metni, J.-M. Pflimlin, T. Hamel, and P. Soueres, "Attitude and gyro bias estimation for a flying UAV," in *IEEE/RSJ Int. Conf. on Intelligent Robots and Systems*, pp. 1114– 1120, 2005.

[9] A. Baerveldt and R. Klang, "A low-cost and low-weight attitude estimation system for an autonomous helicopter," in *IEEE Int. Conf. Intelligent Engineering Systems*, pp. 391–395, 1997.

[10] C. Deeg, M. Musial, and G. Hommel, "Control and simualtion of an autonomously flying model helicopter," in *Proceedings of the 5th IFAC Symposium on Intelligent Autonomous Vehicles*, July 2004.